



CAP2 deficiency delays myofibril actin cytoskeleton differentiation and disturbs skeletal muscle architecture and function

Lara-Jane Kepser^a, Fidan Damar^a, Teresa De Cicco^b, Christine Chaponnier^c, Tomasz J. Prószynski^b, Axel Pagenstecher^d, and Marco B. Rust^{a,e,f,1}

^aMolecular Neurobiology Group, Institute of Physiological Chemistry, University of Marburg, 35032 Marburg, Germany; ^bLaboratory of Synaptogenesis, Nencki Institute of Experimental Biology PAS, 02-093 Warsaw, Poland; ^cDepartment of Pathology and Immunology, University of Geneva, 1211 Geneva, Switzerland; ^dInstitute of Neuropathology, University of Marburg, 35032 Marburg, Germany; ^eCenter for Mind, Brain and Behavior, Research Campus of Central Hessen, 35032 Marburg, Germany; and ^fDFG Research Training Group "Membrane Plasticity in Tissue Development and Remodeling," GRK 2213, University of Marburg, 35032 Marburg, Germany

Edited by Yale E. Goldman, University of Pennsylvania/PMI, Philadelphia, PA, and approved March 14, 2019 (received for review August 7, 2018)

Actin filaments (F-actin) are key components of sarcomeres, the basic contractile units of skeletal muscle myofibrils. A crucial step during myofibril differentiation is the sequential exchange of α -actin isoforms from smooth muscle (α -SMA) and cardiac (α -CAA) to skeletal muscle α -actin (α -SKA) that, in mice, occurs during early postnatal life. This " α -actin switch" requires the coordinated activity of actin regulators because it is vital that sarcomere structure and function are maintained during differentiation. The molecular machinery that controls the α -actin switch, however, remains enigmatic. Cyclase-associated proteins (CAP) are a family of actin regulators with largely unknown physiological functions. We here report a function for CAP2 in regulating the α -actin exchange during myofibril differentiation. This α -actin switch was delayed in systemic CAP2 mutant mice, and myofibrils remained in an undifferentiated stage at the onset of the often excessive voluntary movements in postnatal mice. The delay in the α -actin switch coincided with the onset of motor function deficits and histopathological changes including a high frequency of type IIB ring fibers. Our data suggest that subtle disturbances of postnatal F-actin remodeling are sufficient for predisposing muscle fibers to form ring fibers. Cofilin2, a putative CAP2 interaction partner, has been recently implicated in myofibril actin cytoskeleton differentiation, and the myopathies in cofilin2 and CAP2 mutant mice showed striking similarities. We therefore propose a model in which CAP2 and cofilin2 cooperate in actin regulation during myofibril differentiation.

ringbinden | spiral annulets | actin dynamics | 6p22.3 | Srv2

Ring fibers are muscle fibers containing myofibrils in a perpendicular orientation to the main group of normal, longitudinally orientated myofibrils (1, 2). In cross-sections, ring fibers show circular myofibrils around or serpentine myofibrils crossing the normally orientated myofibrils. Ring fibers have been reported for congenital myopathies (e.g., myotonic dystrophy, limb-girdle dystrophy, inclusion body myositis), for myopathies of unknown etiology (3–5), and for disease mouse models (6, 7). While previous studies suggested the involvement of hypertonic muscle state, aberrant synthesis of myofibril proteins, or cytoskeletal defects (7, 8), the natural cause of ring fiber formation remained elusive.

Cyclase-associated proteins (CAPs) are evolutionary conserved proteins with largely unknown physiological function. CAPs interact with monomeric and filamentous actin, suggesting a role in actin dynamics, the spatiotemporally controlled F-actin assembly and disassembly (9). Indeed, CAP1 and its yeast homolog Srv2 mediated fast F-actin disassembly in vitro (10), and CAP1 accelerates ADF/cofilin-mediate F-actin disassembly in nonmuscle cells (11). Most species express only a single CAP isoform, but vertebrates have two family members, CAP1 and CAP2, encoded by distinct genes (9). Expression of CAP2 is restricted to only a few tissues including brain and striated muscles (11, 12), where it may

have acquired specific functions. While previous analyses of mutant mice demonstrated a role of CAP2 in neuron morphology and heart physiology (13–15), its function in skeletal muscles has not been investigated, yet.

We here report a function for CAP2 in skeletal muscle development. We found that CAP2 controls the exchange of α -actin isoforms during myofibril differentiation. In systemic CAP2-deficient mice, the " α -actin switch" was delayed and coincided with motor function deficits and a myopathy characterized by a large number of ring fibers in type IIB muscle fibers. Our findings highlight CAP2 as a regulator of myofibril actin cytoskeleton differentiation that is critical for skeletal muscle structure and function.

Results

Delayed Maturation of Motor Functions and Reduced Muscle Strength in CAP2 Mutants. To generate CAP2-deficient mice (KO), we intercrossed heterozygous mutants (HET) obtained from the European Conditional Mouse Mutagenesis Program (EUCOMM). Genotyping at postnatal week 2–3 revealed 24% KO among all offspring ($n = 77$), demonstrating that KO were viable and born at

Significance

Displaced myofibrils termed ring fibers have been reported for human congenital myopathies and for myopathies of unknown etiology, but their natural cause largely remained elusive. Cyclase-associated protein 2 (CAP2) is an actin regulator with unknown physiological function. We identified CAP2 as a regulator for the exchange of α -actin isoforms during myofibril differentiation. In CAP2 mutant mice, myofibrils remained in an undifferentiated stage at the onset of excessive voluntary muscle contractions, predisposing them to form ring fibers that compromise skeletal muscle function. Our data confirm that subtle cytoskeletal changes can cause ring fibers. Moreover, they led us to propose that CAP2 inactivation contributes to defects of human 6p22.3 deletion syndrome such as developmental delay and hypotonia.

Author contributions: L.-J.K., T.J.P., A.P., and M.B.R. designed research; L.-J.K., F.D., T.D.C., and A.P. performed research; C.C. contributed new reagents/analytic tools; L.-J.K. and M.B.R. analyzed data; and A.P. and M.B.R. wrote the paper.

The authors declare no conflict of interest.

This article is a PNAS Direct Submission.

This open access article is distributed under [Creative Commons Attribution-NonCommercial-NoDerivatives License 4.0 \(CC BY-NC-ND\)](https://creativecommons.org/licenses/by-nc-nd/4.0/).

¹To whom correspondence should be addressed. Email: marco.rust@staff.uni-marburg.de.

This article contains supporting information online at www.pnas.org/lookup/suppl/doi:10.1073/pnas.1813351116/-DCSupplemental.

Published online April 8, 2019.

the expected Mendelian ratio. To study whether CAP2 inactivation compromised postnatal development, we assessed physical landmarks and developmental milestones in newborn mice. Occurrence of eye opening or pinna detachment as well as activity was similar to wild-type (WT) littermates (Fig. 1 A–C), excluding severe developmental defects in KO. However, KO showed higher tremor levels in particular between postnatal days (P) 10 and 18 (Fig. 1D). Moreover, KO displayed a delayed maturation in motor function tests including surface righting, level screen, vertical screen, negative geotaxis, or bar holding (Fig. 1 E–I and Movie S1). Motor deficits were similar in male and female KO, and we therefore pooled data of both sexes. Motor skills were not impaired in HET. Notably, KO performed similar to WT in other tests that evaluated visual and auditory performance, tactile perception, or reflexes (Fig. 1 J–O). Together, male and female KO showed normal activity, sensation, and reflexes, while maturation of motor functions was delayed. We conclude that CAP2 is specifically relevant for motor function development.

To test whether motor functions were impaired at later stages, we performed the string test that measures forelimb strength by determining the time mice need to pull themselves up when hanging on a bar (16). This latency was increased in both juvenile

(3–4 wk) and adult (6–8 wk) KO (SI Appendix, Fig. S1A). We also determined maximal force generation by performing the grip strength (GS) test. Because KO body weight (BW) was reduced by roughly 20% throughout development (SI Appendix, Fig. S1B), we normalized GS to BW. Normalized GS of either the forepaws or all four paws was reduced by 25% in juvenile and 20% in adult KO (SI Appendix, Fig. S1C and D). KO showed normal motor coordination in the rotarod and normal locomotor activity and exploratory behavior in the open field (SI Appendix, Fig. S1E–G), reflecting their overall healthy appearance. Hence, juvenile and adult KO displayed specific defects in muscle strength.

Myopathy in CAP2 Mutants Is Characterized by Frequent Ring Fibers.

We found CAP2 present in all WT skeletal muscles tested (Fig. 2A). We therefore tested whether muscle weakness was associated with altered muscle histology. In KO, skeletal muscles did not appear atrophic (Fig. 2B), which was also evident from normal weight of the *Musculus (M.) quadriceps femoris* (QUAD; SI Appendix, Fig. S2A). We studied skeletal muscle histology by performing a thorough analysis of cross-sectioned adult QUAD. Hematoxylin-eosin (HE) staining revealed an overall normal QUAD architecture in KO, but we noted a 12-fold increase in

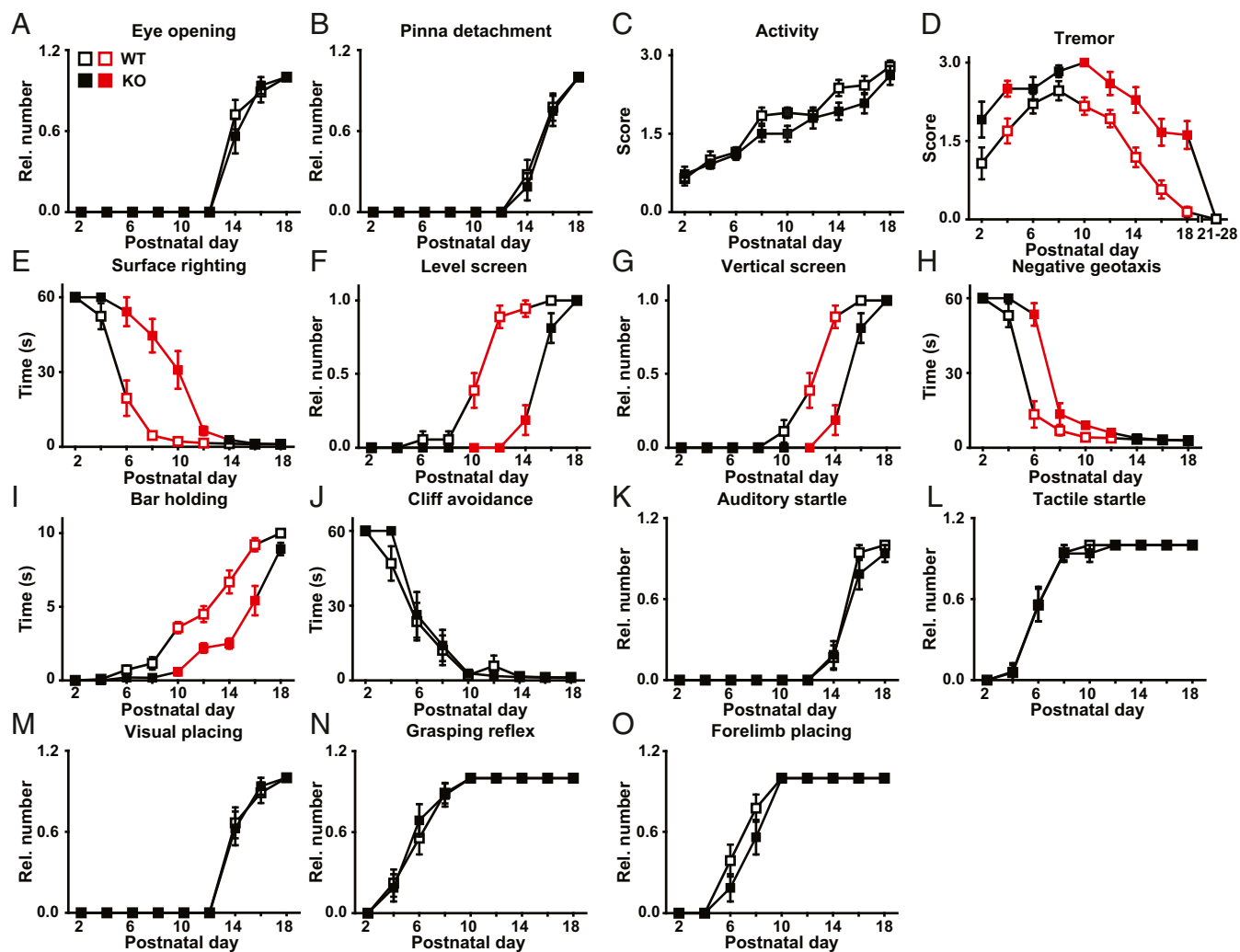


Fig. 1. Motor function deficits in neonatal CAP2 mutants. (A–C) Graphs showing that eye opening, pinna detachment, and activity were unchanged in CAP2 mutants. (D) Instead, CAP2 mutants showed increased levels of tremulous movements. (E–I) Moreover, they performed weaker in various motor function tests. (J–O) No changes were noted in cliff avoidance, auditory startle, tactile startle, visual placing, grasping reflex, or forelimb placing. For A–O: $n = 18$ WT and 16 KO. If mean values (MV) were significantly different between groups ($P < 0.05$), squares indicating MV and error bars indicating SEMs are shown in red.

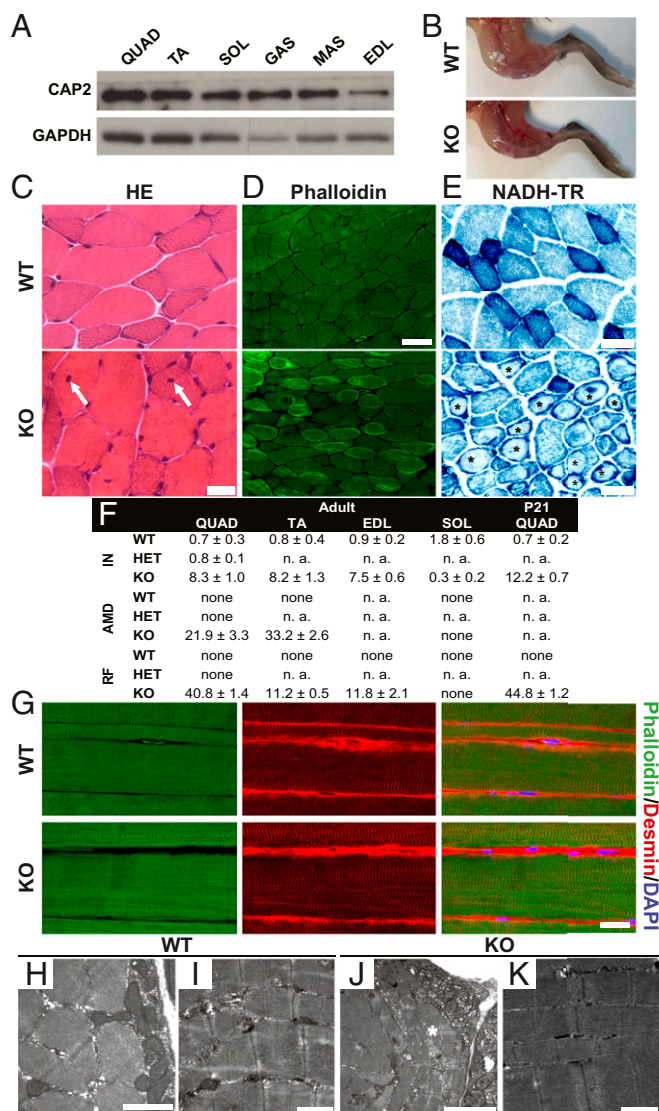


Fig. 2. Myopathy in CAP2 mutants. (A) Immunoblots demonstrating presence of CAP2 in all skeletal muscles tested (GAS, *M. gastrocnemius*; MAS, *M. masseter*). GAPDH was used as a loading control. (B) Micrographs showing skinned hind legs from age-matched WT and KO. (C) HE-stained adult QUAD cross-sections. White arrows indicate internalized nuclei in KO. (D) Phalloidin staining revealed frequent occurrence of ring fibers in KO. (E) NADH-TR staining revealed altered mitochondrial distribution in KO (asterisks). (F) Quantification of histopathological changes in adult skeletal muscles and in P21 QUAD. Muscle fibers (%) with internalized nuclei (IN), altered mitochondrial distribution (AMD), and ring fibers (RF). n.a., not analyzed. For each analysis, at least nine micrographs of 0.6 mm² from three mice per genotype have been used. (G) Antibody staining against desmin (red) in longitudinal TA sections. Sections were counterstained with phalloidin (green) and Hoechst 33342 (blue). (H–K) EM of adult WT and KO QUAD cross- and longitudinal sections. Asterisk in J indicates a ring fiber. Scale bar (μm): 1.0 (H, I, and K), 2.5 (J), 20 (C and G), 50 (D), 30 (E).

the fraction of internalized nuclei and the occurrence of ring fibers (Fig. 2C and *SI Appendix*, Fig. S2B). We exploited fluorescent phalloidin that labels F-actin to better visualize ring fibers and confirmed their presence in 41% of muscle fibers (Fig. 2D and F and *SI Appendix*, Fig. S2C). In QUAD cross-sections, ring fibers were equally distributed. Staining of sequential sections with either phalloidin or antibodies against myosin heavy chain (MHC) isoforms revealed presence of ring fibers in MHC IIB-labeled, but not in MHC IIA-labeled muscle fibers (*SI Appendix*, Fig. S2E and

F). MHC isoform-specific antibodies further allowed a quantification of fiber-type fractions, which was unchanged in KO (*SI Appendix*, Fig. S2G). Staining of nicotinamide adenine dinucleotide tetrazolium reductase (NADH-TR) or succinate dehydrogenase/cytochrome oxidase II (SDH/COXII) revealed that mitochondrial distribution was severely disturbed in 22% of muscle fibers (Fig. 2E and F and *SI Appendix*, Fig. S3A). A closer inspection revealed a normal number of intensively labeled “oxidative” (type I) muscle fibers in KO QUAD, suggesting that altered mitochondrial distribution was present in lighter “less oxidative” (type II) muscle fibers, which are mainly of type IIB (*SI Appendix*, Fig. S2G). Gömöri trichrome staining confirmed the presence of internalized nuclei, and ATPase and periodic acid-Schiff (PAS) staining confirmed the occurrence of ring fibers (*SI Appendix*, Figs. S2D and S3B–C). Apart from that, we did not find any additional changes in Gömöri trichrome staining, PAS staining, oil red O staining, van Gieson’s staining, or acid phosphatase staining (*SI Appendix*, Fig. S3B–F), thereby demonstrating the absence of lipid deposits or macrophages as well as normal patterns of glycogen and connective tissue in KO mice. In summary, our QUAD analyses revealed internalized nuclei, disturbed mitochondrial distribution, and a high frequency of ring fibers that were restricted to type IIB muscle fibers. Histopathological changes were very similar in QUAD from female and male KO, while no such changes were present in HET (*SI Appendix*, Fig. S4). We further analyzed *M. tibialis anterior* (TA), *M. soleus* (SOL), and *M. extensor digitorum longus* (EDL). Similar to QUAD, type IIB muscle fibers predominate in TA and EDL (17). Instead, type I and IIA muscle fibers predominate in SOL, which do not possess type IIB muscle fibers. Very similar to QUAD, we frequently found ring fibers, internalized nuclei, and muscle fibers with disturbed mitochondrial distribution in TA and EDL (Fig. 2F and *SI Appendix*, Figs. S5 and S6). Conversely, the number of internalized nuclei was not increased in SOL, and we did not find ring fibers or mitochondrial distribution defects. Together, histopathological changes were present in all “type IIB muscle fiber predominated” skeletal muscles examined, but not in SOL.

We next performed immunohistochemistry on longitudinal sections to examine sarcomere structure. We performed these experiments on TA, in which immunohistochemistry was superior to QUAD. Phalloidin staining revealed a regular striated F-actin pattern that was very similar in WT and KO (Fig. 2G). We confirmed an overall normal sarcomere structure in KO by antibody staining against desmin that surrounds Z-discs. To characterize muscle fibers on the ultrastructural level, we performed electron microscopy (EM) on adult QUAD (Fig. 2H–K). EM confirmed both presence of ring fibers in numerous KO muscle fibers as well as subsarcolemmal accumulation of mitochondria. Moreover, sarcomere ultrastructure appeared normal in KO QUAD. Hence, KO myopathy was not associated with obvious defects in sarcomere structure.

CAP2 Controls Postnatal Skeletal Muscle Differentiation. Because motor function deficits were present in KO neonates, we tested developmental CAP2 expression in skeletal muscles and found similar levels throughout QUAD development (Fig. 3A). We therefore tested whether onset of myopathy coincided with motor function deficits in neonatal KO. We noted no differences between WT and KO QUAD cross-sections at P4 (Fig. 3B). Instead, ring fibers were present during the second postnatal week. They appeared together with phalloidin-labeled, F-actin-rich aggregates that were not present at later stages (P21, adult). Phalloidin and HE staining at P21 revealed frequent occurrence of ring fibers and internalized nuclei, very similar to adult QUAD (Figs. 2F and 3B and *SI Appendix*, Fig. S7A). EM analyses on QUAD longitudinal and cross-sections confirmed the presence of ultrastructural changes at P8 including irregular arrangement of myofibrils and abnormal distribution of mitochondria, as well as the occasional

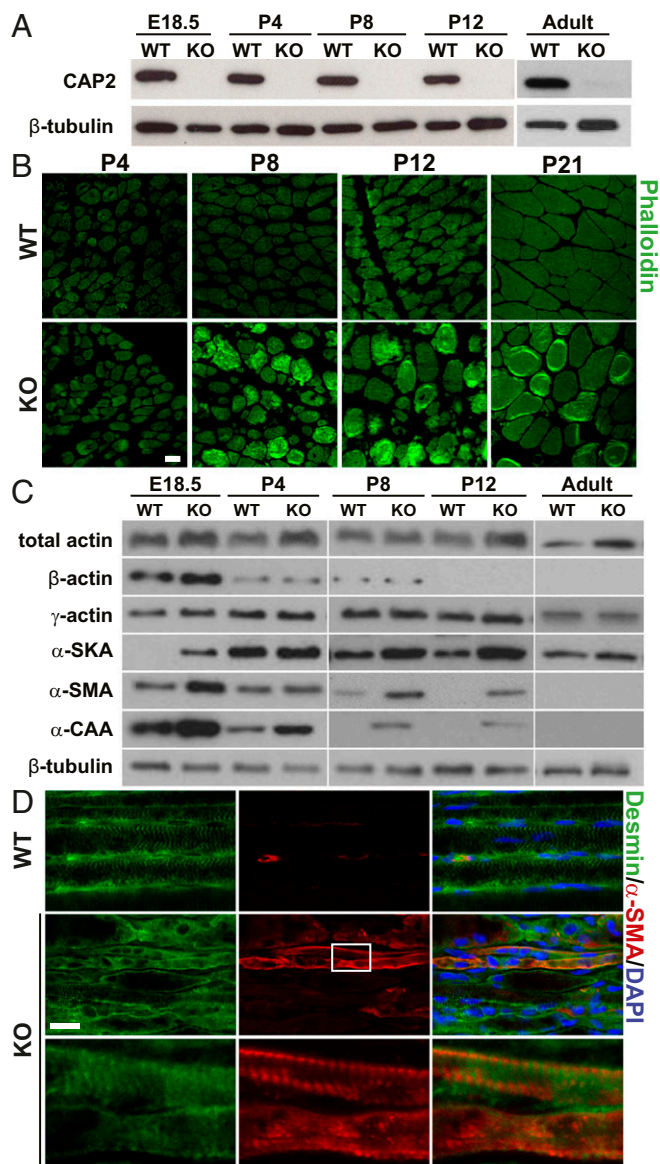


Fig. 3. Myopathy onset coincides with delay in α -actin switch. (A) Immunoblots demonstrating CAP2 expression throughout QUAD development. β -tubulin was used as a loading control. (B) Micrographs showing phalloidin-stained QUAD cross-sections. (C) Immunoblots showing levels of total actin (pan-actin), skeletal muscle (α -SKA), smooth muscle (α -SMA), and cardiac α -actin (α -CAA), β -actin, and γ -actin throughout QUAD development. β -tubulin was used as a loading control. (D) Antibody staining against desmin (green) and α -SMA (red) in longitudinal TA sections from P12 mice. Sections were counterstained with DAPI (blue). White box indicates area in KO TA shown at higher magnification. Scale bars (μ m): 20 (B and D).

occurrences of abnormal undulation of Z-bands, dilated tubulus systems, and subsarcolemmal accumulation of lipid droplets (*SI Appendix, Fig. S7 B–K*). Together, histopathology started during the first week of life and coincided with the onset of motor dysfunction. These findings reveal a pivotal function of CAP2 for early postnatal skeletal muscle development.

A crucial step during early postnatal skeletal muscle development is the replacement of smooth muscle (α -SMA) and cardiac muscle (α -CAA) α -actin by skeletal muscle (α -SKA) α -actin (18, 19). This exchange requires the coordinated release of actin subunits, and cofilin2, a putative CAP2 interaction partner (9), has been implicated therein (20). To test whether CAP2 is critical for

this exchange, we quantified levels of α -actin isoforms by exploiting isoform-specific antibodies (21). Additionally, a pan-actin antibody was used to assess total actin levels. Compared with WT, total actin levels were higher in KO at all postnatal stages examined and remained increased in adult mice (Fig. 3C). This increase was due to elevated α -actin because β -actin and γ -actin levels were unchanged. Indeed, compared with controls, α -SKA levels were higher in KO throughout development. In WT, α -SMA and α -CAA levels gradually declined postnatal, similar to previous studies (20). However, their decline was delayed in KO. Consequently, α -SMA and α -CAA levels were elevated at postnatal stages and still detectable in P12 KO (Fig. 3C). In sharp contrast to elevated protein levels, mRNA levels of *Acta1*, *Acta2*, and *Actc1*, which encode α -SKA, α -SMA, and α -CAA, respectively, were reduced at E18.5, but unaltered at P4 (*SI Appendix, Fig. S8 A and B*). Hence, elevated protein levels in KO were not caused by increased gene expression. We therefore suspected a delayed removal from F-actin and degradation of α -SMA and α -CAA. If this holds true, α -SMA and α -CAA should be present in the F-actin-enriched insoluble protein fraction in P12 KO. To test this, we separated soluble (containing actin monomers) and insoluble protein fractions and determined levels of α -actin isoforms in both fractions. As expected, the majority of α -SKA was found in the insoluble WT fraction, and we found a very similar distribution in KO (*SI Appendix, Fig. S8C*). However, while α -SMA and α -CAA were not detectable in either WT fraction, the vast majority of both proteins was present in the insoluble KO fraction. These data suggested that α -SMA and α -CAA were still integrated in F-actin in P12 KO. To prove this, we performed antibody staining on longitudinal TA sections. In this analysis, we were limited to α -SMA because of unspecific α -CAA signals. As expected, α -SMA immunoreactivity was restricted to blood vessels in P12 WT (Fig. 3D). Conversely, we frequently found α -SMA-positive muscle fibers in KO. Notably, these muscle fibers showed a striated α -SMA pattern, demonstrating that α -SMA was an integral component of sarcomere F-actin. Together, our data revealed a delayed α -actin switch in KO sarcomeres, and they implicated CAP2 in the exchange of α -actin isoforms during myofibril differentiation.

CAP2 Reexpression Rescues Ring Fiber Myopathy in CAP2 Mutants.

Because the delayed α -actin switch coincided with the onset of ring fibers, we hypothesized that the pathology was caused by a primary defect in skeletal muscles. To test our hypothesis, we reexpressed GFP-CAP2 in KO QUAD by viral transduction at P0, before onset of myopathy, and killed mice at P21 to screen for ring fibers that we used as a readout (Fig. 4A). In this experiment, expression of GFP-CAP2 was restricted to peripheral QUAD regions (Fig. 4B), which allowed us to compare ring fiber formation between CAP2 reexpressing and CAP2-deficient muscle fibers in the same QUAD. We additionally performed control experiments, in which we expressed GFP in KO QUAD. As expected, the fraction of muscle fibers with ring fibers was independent of GFP expression in control KO QUAD (Fig. 4C). Similarly, ring fibers were frequently present in KO muscle fibers not expressing GFP-CAP2. Conversely, we hardly found any ring fibers in GFP-CAP2 expressing muscle fibers in KO QUAD. These findings proved our hypothesis that loss of CAP2 activity in skeletal muscles caused ring fiber myopathy in KO.

Discussion

In the present study, we report a function for the actin regulator CAP2 in skeletal muscle development. We found that CAP2 is crucial for the exchange of α -actin isoforms during myofibril differentiation. In CAP2 mutant mice, this α -actin switch was delayed and coincided with the onset of a myopathy characterized by type IIB ring fibers and motor dysfunction. Rescue experiments in alive mutants proved that loss of CAP2 activity in skeletal muscles caused the myopathy. Our data indicate that the

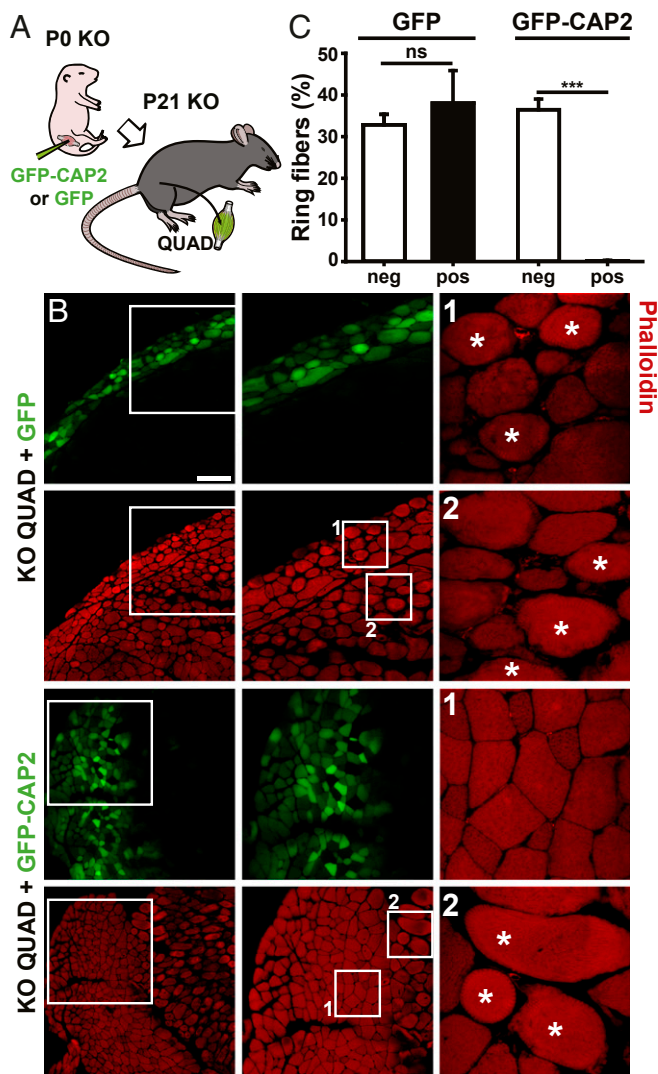


Fig. 4. CAP2 reexpression rescued ring fiber myopathy in KO. (A) Scheme showing experimental approach for rescue experiments in KO QUAD. (B) Micrographs from P21 KO QUAD cross-sections upon viral transduction of either GFP or GFP-CAP2. Sections were counterstained with phalloidin (red) to screen for ring fibers. White boxes indicate areas shown at higher magnification. Asterisks indicate ring fibers. Scale bar (μm): 100. (C) Graph showing fractions of GFP-negative or GFP-positive muscle fibers displaying ring fibers in P21 KO QUAD upon viral induction of either GFP or GFP-CAP2. GFP: negative, $32.8 \pm 1.8\%$; positive, $38.0 \pm 5.5\%$, $P = 0.547$. GFP-CAP2: negative, $36.5 \pm 2.3\%$; positive, 0.2 ± 0.1 , $P < 0.001$. $n = 6$ images from three mice. $\text{MV} \pm \text{SEM}$ are shown in C. ns, not significant, $***P < 0.001$.

early postnatal period constitutes a vulnerable phase, in which delayed differentiation of the sarcomere actin cytoskeleton leads to the development of ring fibers.

Apart from ring fibers, KO displayed an elevated number of internalized nuclei and a disturbed distribution of mitochondria. While sarcomere structure was preserved in the majority of muscle fibers, we only very rarely noted moderate Z-band streaming. Accordingly, we did not find Z-band protein-containing remnants (nemaline bodies, ref. 22). KO skeletal muscles did not appear atrophic, and they showed a normal fiber-type proportion. Further, we did not find inclusion bodies, myofibrillar accumulations, sarcoplasmic bodies, (central) cores, fiber necrosis, increased connective tissue, or fat cells—characteristic features for myopathies including myofibrillar myopathies, inclusion body myopathy, central core disease, or dystrophies. Hence, a large fraction of ring

fibers characterized the myopathy in CAP2 mutants. Myopathic changes became apparent during early postnatal life, increased until the third postnatal week, and were stable thereafter. Likewise, motor function deficits were present in newborn mutants, and muscle weakness was similar in juvenile and young adult mutants. Our data imply that CAP2 is relevant specifically for skeletal muscle development. The inheritance of the pathological phenotype is autosomal recessive, since HET were indistinguishable from WT.

What could cause ring fiber formation in CAP2 mutants? One important aspect of myofibril differentiation is the assembly and precise alignment of F-actin (23). This includes the sequential exchange of α -actin isoforms that, in mice, occurs during early postnatal life (*SI Appendix, Fig. S9A*, refs. 18 and 19). Specifically, α -SKA replaces α -SMA and α -CAA to become the major α -actin in differentiated myofibrils. This α -actin switch requires the coordinated release of actin subunits (20), a process that might depend on proper function of CAP2. In agreement with recent literature (20), we observed a gradual increase of α -SKA in skeletal muscles during early postnatal life and a concomitant decline in α -CAA and α -SMA levels, which were both absent from WT at P12. At this stage, substantial levels of α -CAA and α -SMA were still present in KO. The striated pattern of α -SMA immunoreactivity in muscle fibers, together with its occurrence in the insoluble protein fraction indicated that α -SMA was an integral component of sarcomere F-actin in mutant myofibrils at P12. Notably, α -CAA distribution between soluble and insoluble protein fractions was similar to α -SKA or α -SMA in P12 KO, suggesting that α -CAA was also a component of F-actin. Together, we found a delayed α -actin switch in mutant sarcomeres, suggesting that mutant myofibrils remained in an undifferentiated stage at the onset of the often excessive voluntary muscle contraction around P10 (24). Hence, we identified CAP2 as a critical α -actin exchange factor during myofibril differentiation. A similar function has been proposed for cofilin2 (20), and the myopathy in cofilin2 mutant mice showed some similarities to that of CAP2 mutants (20, 25). We therefore propose a model in which CAP2 and cofilin2 cooperate in regulating the exchange of α -actin isoforms during myofibril differentiation (*SI Appendix, Fig. S9B*). In line with our model, a cooperative activity in F-actin turnover in nonmuscle cells has been shown for their close homologs CAP1 and cofilin1 (11, 26), which share similar biochemical functions with CAP2 and cofilin2, respectively (9, 27).

Could a delayed α -actin switch explain the myopathy in KO? Previous studies reported functional differences between myofibrils containing either α -CAA or α -SKA, although both α -actin isoforms are 99% identical and vary only at four amino acid residues (28). They showed that (i) force generation in isolated cardiac myofibrils was fourfold smaller than in skeletal muscle myofibrils, (ii) heart contractility was increased in BALB/c mice expressing unusual low α -CAA and high α -SKA levels, and (iii) maximal specific force was reduced in α -SKA null mice expressing α -CAA in skeletal muscles (29–32). Importantly, *in vitro* studies further demonstrated that α -CAA filaments were less stable than α -SKA filaments (33). In WT, the switch to the more stable α -SKA that exerts higher mechanical force occurs before mice start strong voluntary movements and in particular pass through the phase of hopping movements during the second to third postnatal week (24). In CAP2-deficient mice, the retarded α -actin switch leads to the simultaneous presence of all three α -actin isoforms in skeletal muscle during this phase of sharply increasing force exertion. We propose that undifferentiated, α -SMA- and α -CAA-containing myofibrils disrupted and reassembled in a random manner thereby leading to ring fibers. This scenario would also explain our observation that ring fibers were restricted to fast twitching type IIB muscle fibers that, compared with type I or IIA fibers, are exposed to higher mechanical forces during muscle contraction (34). In line with this scenario, type IIB ring fiber have been reported for transgenic mice expressing a mutant α -SKA variant that weakened

the interaction between actin subunits (7). Hence, our data and other studies suggest that subtle changes in sarcomere F-actin composition increase the vulnerability of muscle fibers to form ring fibers.

In summary, our study unraveled a critical function for CAP2 in refining the actin cytoskeleton during myofibril differentiation. Given that skeletal muscle differentiation is similar in humans, we propose a crucial function for CAP2 in human myofibril differentiation. In fact, transgenic mouse lines displayed myopathies similar to those associated with mutations in human actin-related genes (7, 25, 35). We therefore propose that mutations in human CAP2 gene may cause ring fiber myopathy. Notably, human CAP2 has been localized to 6p22.3, and interstitial deletions of variable sizes encompassing the CAP2 locus have been associated with clinical symptoms including developmental delay, hypotonia, and heart defects (36–38). While we showed here developmental delay and hypotonia for CAP2 mutant mice, others previously reported heart defects (13, 14, 39). We therefore propose that loss of CAP2 causes or contributes to the pathology of 6p22.3 deletion syndrome.

Materials and Methods

Mice. CAP2 mutants were obtained from the European Conditional Mouse Mutagenesis Program (EUCOMM). See *SI Appendix* for more information on mice and their husbandry. Behavioral experiments and killing of mice were approved by internal animal welfare authorities of the University of Marburg and the Regierungspräsidium Giessen (references: AK-6-2014-Rust, V54-19c2015h01M20/29 Nr. G27/2016, V54-19c2015h01M20/30 Nr. G65/2016). Virus infection was approved by the First Warsaw Local Ethics Committee for Animal Experimentation (reference: 36/2017).

- Banker BQ, Engel AG (1986) Basic reactions of muscle. *Myology. Basic and Clinical*, eds Banker BQ, Engel AG (McGraw-Hill, New York), pp 845–907.
- Carpenter S, Karpati G (1984) *Pathology of Skeletal Muscle* (Churchill Livingstone, New York), pp 216–220.
- Bethlem J, Vanwijngaarden GK (1963) The incidence of ringed fibres and sarcoplasmic masses in normal and diseased muscle. *J Neurol Neurosurg Psychiatry* 26:326–332.
- Del Bigio MR, Jay V (1992) Inclusion body myositis with abundant ring fibers. *Acta Neuropathol* 85:105–110.
- Joyce NC, Oskarsson B, Jin LW (2012) Muscle biopsy evaluation in neuromuscular disorders. *Phys Med Rehabil Clin N Am* 23:609–631.
- Mankodi A, et al. (2000) Myotonic dystrophy in transgenic mice expressing an expanded CUG repeat. *Science* 289:1769–1773.
- Ravenscroft G, et al. (2011) Mouse models of dominant ACTA1 disease recapitulate human disease and provide insight into therapies. *Brain* 134:1101–1115.
- Peña J, Luque E, Noguera F, Jimena I, Vaamonde R (2001) Experimental induction of ring fibers in regenerating skeletal muscle. *Pathol Res Pract* 197:21–27.
- Ono S (2013) The role of cyclase-associated protein in regulating actin filament dynamics - more than a monomer-sequestration factor. *J Cell Sci* 126:3249–3258.
- Johnston AB, Collins A, Goode BL (2015) High-speed depolymerization at actin filament ends jointly catalyzed by Twinfilin and Srv2/CAP. *Nat Cell Biol* 17:1504–1511.
- Bertling E, et al. (2004) Cyclase-associated protein 1 (CAP1) promotes cofilin-induced actin dynamics in mammalian nonmuscle cells. *Mol Biol Cell* 15:2324–2334.
- Peche V, et al. (2007) CAP2, cyclase-associated protein 2, is a dual compartment protein. *Cell Mol Life Sci* 64:2702–2715.
- Peche VS, et al. (2013) Ablation of cyclase-associated protein 2 (CAP2) leads to cardiomyopathy. *Cell Mol Life Sci* 70:527–543.
- Field J, et al. (2015) CAP2 in cardiac conduction, sudden cardiac death and eye development. *Sci Rep* 5:17256, and erratum (2016) 6:26640.
- Kumar A, et al. (2016) Neuronal actin dynamics, spine density and neuronal dendritic complexity are regulated by CAP2. *Front Cell Neurosci* 10:180.
- Deacon RM (2013) Measuring motor coordination in mice. *J Vis Exp* 75:e2609.
- Augusto V, Padovani CR, Campos GER (2004) Skeletal muscle fiber types in C57BL/6 mice. *Braz J Morphol Sci* 21:89–94.
- Tondeleir D, Vandamme D, Vandekerckhove J, Ampe C, Lambrechts A (2009) Actin isoform expression patterns during mammalian development and in pathology: Insights from mouse models. *Cell Motil Cytoskeleton* 66:798–815.
- Mizuno Y, Suzuki M, Nakagawa H, Ninagawa N, Torihashi S (2009) Switching of actin isoforms in skeletal muscle differentiation using mouse ES cells. *Histochem Cell Biol* 132:669–672.
- Gurniak CB, et al. (2014) Severe protein aggregate myopathy in a knockout mouse model points to an essential role of cofilin2 in sarcomeric actin exchange and muscle maintenance. *Eur J Cell Biol* 93:252–266.
- Chaponnier C, Gabbiani G (2016) Monoclonal antibodies against muscle actin isoforms: Epitope identification and analysis of isoform expression by immunoblot and immunostaining in normal and regenerating skeletal muscle. *F1000 Res* 5:416.
- Luther PK (2009) The vertebrate muscle Z-disk: Sarcomere anchor for structure and signalling. *J Muscle Res Cell Motil* 30:171–185.

Developmental Milestones. A test battery to assess developmental milestones has been previously described (40). See *SI Appendix* for detailed description.

Histology. Mice were killed by cervical dislocation or decapitation. Upon dissection, skeletal muscle specimens were snap-frozen in isopentane-cooled liquid nitrogen and stored at -80°C until further processing. Histochemical stains were performed as described (41). See *SI Appendix* for detailed description and antibody list.

Electron Microscopy. EM was performed as described (42). See *SI Appendix* for detailed description.

Immunoblot Analyses. See *SI Appendix* for a detailed description of methods and a list of all antibodies.

Virus Production and Pup Treatment. See *SI Appendix* for a detailed description.

Statistics. Significance was calculated using Student's *t* test. All experiments were conducted by experimenters blind to the genotype. If not specified (histology, immunoblots), all experiments have been conducted in at least three independent experiments (three biological replicates).

ACKNOWLEDGMENTS. We thank the EUCOMM for providing CAP2 mutant mice; Katja Gessner and Isabell Metz for generating graphical schemes; and Karlheinz Burk, Bettina Kowalski, Denis Grabski, Sylvia Stanek, and Heidrun Jennemann for excellent technical support. L.-J.K. was supported by the DFG Research Training Group 2213 “Membrane Plasticity in Tissue Development and Remodeling.” This work was supported by a research grant (MR 24/20147) from the University Medical Center Giessen Marburg (UKGM) and by a research grant (ACAciA) from the Fondazione Cariplo (to M.B.R.), as well as a grant from Polish National Science Center (UMO-2016/21/B/NZ3/03638) (to T.J.P.).

- Ono S (2010) Dynamic regulation of sarcomeric actin filaments in striated muscle. *Cytoskeleton (Hoboken)* 67:677–692.
- Fuller JL, Wimer RE (1966) Neural, sensory, and motor functions. *Biology of the Laboratory Mouse*, ed Green EL (Dover Publ, New York), 2nd Ed.
- Agrawal PB, Joshi M, Savic T, Chen Z, Beggs AH (2012) Normal myofibrillar development followed by progressive sarcomeric disruption with actin accumulations in a mouse Cfl2 knockout demonstrates requirement of cofilin-2 for muscle maintenance. *Hum Mol Genet* 21:2341–2356.
- Moriyama K, Yahara I (2002) Human CAP1 is a key factor in the recycling of cofilin and actin for rapid actin turnover. *J Cell Sci* 115:1591–1601.
- Hild G, Kalmár L, Kardos R, Nyitrai M, Bugyi B (2014) The other side of the coin: Functional and structural versatility of ADF/cofilins. *Eur J Cell Biol* 93:238–251.
- Chaponnier C, Gabbiani G (2004) Pathological situations characterized by altered actin isoform expression. *J Pathol* 204:386–395.
- Linke WA, Popov VI, Pollack GH (1994) Passive and active tension in single cardiac myofibrils. *Biophys J* 67:782–792.
- Hewett TE, Grupp IL, Grupp G, Robbins J (1994) Alpha-skeletal actin is associated with increased contractility in the mouse heart. *Circ Res* 74:740–746.
- Jackaman C, et al. (2007) Novel application of flow cytometry: Determination of muscle fiber types and protein levels in whole murine skeletal muscles and heart. *Cell Motil Cytoskeleton* 64:914–925.
- Nowak KJ, et al. (2009) Rescue of skeletal muscle alpha-actin-null mice by cardiac (fetal) alpha-actin. *J Cell Biol* 185:903–915.
- Orbán J, Lorinczy D, Nyitrai M, Hild G (2008) Nucleotide dependent differences between the alpha-skeletal and alpha-cardiac actin isoforms. *Biochem Biophys Res Commun* 368:696–702.
- MacIntosh BR, Gardiner PF, McComas AJ (2006) *Skeletal Muscle: Form and Function* (Human Kinetics, Champaign, IL), 2nd Ed.
- Crawford K, et al. (2002) Mice lacking skeletal muscle actin show reduced muscle strength and growth deficits and die during the neonatal period. *Mol Cell Biol* 22:5887–5896.
- Bremer A, Schoumans J, Nordenskjöld M, Anderlid BM, Giacobini M (2009) An interstitial deletion of 7.1Mb in chromosome band 6p22.3 associated with developmental delay and dysmorphic features including heart defects, short neck, and eye abnormalities. *Eur J Med Genet* 52:358–362.
- Celestino-Soper PB, et al. (2012) Deletions in chromosome 6p22.3-p24.3, including ATXN1, are associated with developmental delay and autism spectrum disorders. *Mol Cytogenet* 5:17.
- Di Benedetto D, et al. (2013) 6p22.3 deletion: Report of a patient with autism, severe intellectual disability and electroencephalographic anomalies. *Mol Cytogenet* 6:4.
- Stöckigt F, et al. (2016) Deficiency of cyclase-associated protein 2 promotes arrhythmias associated with connexin43 maldistribution and fibrosis. *Arch Med Sci* 12:188–198.
- Heyser CJ (2004) Assessment of developmental milestones in rodents. *Curr Protoc Neurosci*, Chapter 8, Unit 8.18.
- Dubowitz V, Sewry C, Oldfors A (2013) *Muscle Biopsy: A Practical Approach* (Saunders Ltd., Philadelphia), pp 21–27.
- Kraushaar T, et al. (2015) Interactions by the fungal Flo11 adhesin depend on a fibronectin type III-like adhesin domain girdled by aromatic bands. *Structure* 23:1005–1017.